Analysis of 1x4 Power Combiner with Rectangular Slot for Microwave Application

N.S.A.S Ali, M.Z.A. Abd Aziz, B. H Ahmad, Y. E. Masrukin and F. A. Hussin
Centre for Telecommunication Research and Innovation (CeTRI), Faculty of Electronics and Computer Engineering, Universiti Teknikal Malaysia Melaka (UTeM), Hang Tuah Jaya, 76100 Durian Tunggal, Melaka, Malaysia.
nurshaheeraalia@yahoo.com.

***Abstract*—This paper presents the design and analysis of the 1x4 Power Combiner with Rectangular Slot for Microwave Application. The focused frequency ranges were from 0.5 GHz to 6 GHz. Three main parameters were investigated in this paper which was length of slot (L1), width of slot (W1) and position of slot (distance). The numerical analysis had been done on the proposed parametric to characterize the effect. The design of tapered finline in the power combiner was simulated using a CST Microwave Studio Software. The simulation process was based on the input return loss and insertion loss at every input port. The rectangular slot was able to enhance the wideband by approximately 400 MHz.**

***Index Terms*—Tapered Finline; Power Combiner; Rectangular Slot.**

I. INTRODUCTION

In wireless communication systems, particularly transmitter hardware, high-power millimetre-wave power amplifiers were very important in millimetre-wave transmitters. But, they are hard to realize in monolithic microwave integrated circuits (MMICs). To overcome the problem, power-combining technologies have become the attractive solution to construct the millimetre-wave power-combining amplifiers [1]. Power dividers and combiners are widely used in microwave/millimeter-wave circuits for distributing and processing signals as needed, especially in the application of wideband power amplification where output power from an individual device is not enough [2]. Commonly, millimeter-wave solid-state power combining can be separated into four categories which are circuit-level power combining, chip-level power combing, spatial power combining and hybrid type power combining [3]. Many circuit-level combining approaches, such as corporate combining, suffer from increased loss (and, hence, reduced combining efficiency) as the number of devices increases. On the contrary, the loss is relatively independent of the number of devices in a well-designed spatial combiner. As a result, spatial power combining is preferred in certain high power applications requiring a large number of amplifiers [4]. For the implementation of high-power spatial combiners, where the output power is at the level of tens or hundreds of watts, several issues have to be incorporated in the design to achieve the desired performance. When dealing with a large number of high-power amplifiers, thermal management is extremely important since device performance degrades drastically if waste heat cannot be removed efficiently. The combiner must be compact, but large enough (physically and thermally) to accommodate the desired number of amplifiers. Minimizing output combiner losses is also critical as far as combiner efficiency is concerned. It is worth emphasizing that for combiner systems based on high-gain amplifiers, only the loss associated with the output network is important [5]. Previous papers had reported a waveguide-based spatial power-combiner circuit that addressed these issues [6]–[8]. The concept is illustrated schematically in Figure 1 which exploits the inherent spatial distribution of the field energy in the dominant waveguide mode to distribute and collect power to and from a dense array of amplifiers. Transitions between the amplifier and waveguide mode are made via electrically close tapered-slot antennas (or finline structures). The enclosed waveguide provides an excellent heat-sinking environment for the power devices and is a natural choice for most high-power applications [9].

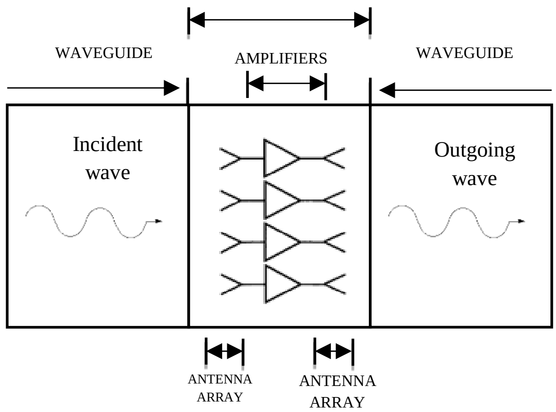

Figure 1: Schematic Diagram

II. POWER COMBINER DESIGN PROCESS

The rectangular waveguide spatial power combining structure proposed consists of a tapered slot (finline structure) are shown in Figure 2. At both ends of the waveguide, a coaxial adapter (input port) and discrete port (output port) provide a standard 50 Ohm SMA connector. In order to couple the energy traveling inside the waveguide structure, some UWB matched transitions need to be designed. Those transitions are defined in the literature as “antennas”, but they are nothing but finlines inserted into the waveguide environment. In this work, exponentially-tapered finline transitions were used. The equations given in [11] for the synthesis of Vivaldi antennas can be used for a preliminary estimation of the taper parameters. The exponential profile curves employed in this structure E1 and, E2 are expressed according to the following functions:

$$y = \pm[C_1 e^{Rx} + C_2] \quad (1)$$

$$C_1 = \frac{y_2 - y_1}{e^{Rx_2} - e^{Rx_1}} \quad (2)$$

$$C_2 = \frac{y_1 e^{Rx_2} - y_2 e^{Rx_1}}{e^{Rx_2} - e^{Rx_1}} \quad (3)$$

where C1 and C2 are the constant and R is the opening rate. The two points P1 (X_1, Y_1) and P2 (X_2, Y_2) is supposedly the beginning and the end points, and Y indicates the distance between the exponential edge and the central axis in the direction perpendicular to the central axis, while X indicates between the edge and bottom of the antenna in the direction parallel to the central axis. The tapered slot (finline structure) consists of two copper layers at the same plane; the first layer (layer 1) is connected to the input port of the feeding line and the second layer (layer 2) is the ground plane. The layers are arrayed to get the 1x4 power combiner. The thickness of copper (*t*) is 0.035mm. Normally, the gradient curve is symmetrical for both layers. The substrate used in this design is FR4. FR4 substrate is used in this design because it is light in weight so it will be easier to fabricate. The design is simulated using an FR4 board with a thickness of 1.6 mm, tangent loss of 0.019 S/m and permittivity of 4.4. There are a few parameters considered for the satisfactory element of the finline structure. The length and width of the taper generally need to be greater than λ_o and $\lambda_o/2$ respectively.

The overall width, length and height of the rectangular casing are presented as Wg, Lg and Hg. Ws, Ls and h are the overall width, length and thickness of the substrate. L1 is the length of taper; W_a, W_b, W_c, and W_d are defined as the slot width and the exponential coefficient are E_1, E_2, E_3, E_4, E_5, E_6, E_7 and E_8. Figure 2 illustrates the basic structure of a 1x4 power combiner. The geometry parameters of the 1x4 power combiner with the rectangular slot are presented in Figure 3 (a) and Figure 3(b) while Table 1 shows the optimized dimensions of the 1x4 power combiner with the rectangular slot.

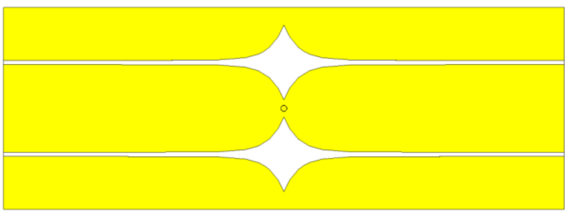

Figure 2: Basic structure of 1x4 Power Combiner

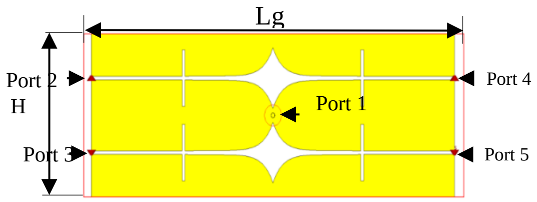

(a) Front view

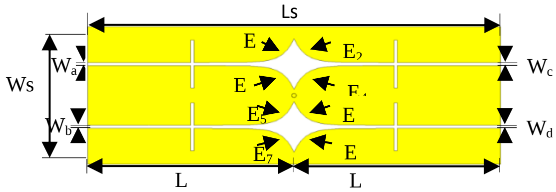

(b) Front view

Figure 3: 1X4 Power Combiner with Rectangular Slot

Table 1
Dimension of Power Combiner

Description	Design Parameter	Value (mm)
Width of waveguide	Wg	10
Height of waveguide	Hg	46
Length of waveguide	Lg	134
Width of substrate	Ws	42
Length of substrate	Ls	128
Length of taper	L	64
Exponential coefficient	E_1	0.3
Exponential coefficient	E_2	0.3
Exponential coefficient	E_3	0.3
Exponential coefficient	E_4	0.3
Exponential coefficient	E_5	0.3
Exponential coefficient	E_6	0.3
Exponential coefficient	E_7	0.3
Exponential coefficient	E_8	0.3
Slot Width	W_a	0.5
Slot Width	W_b	0.5
Slot Width	W_c	0.5
Slot Width	W_d	0.5
Width of slot	W1	5
Length of slot	L1	8
Position of slot	distance	32
Thickness of copper	t	0.035
Thickness of substrate	h	1.6

III. RESULT AND DISCUSSION

The design process is based on a 1x4 power combiner design as shown in Figure 3. A rectangular slot is invented into the design structure to determine the effect. The rectangular slot is investigated based on the position, width and length. Figure 4 shows the geometry of the rectangular slot.

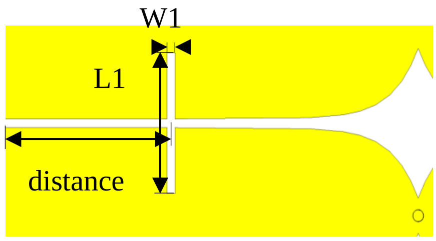

Figure 4: Geometry of Rectangular slot

A. Position of Rectangular Slot

The result in Figure 5 shows the return loss and insertion loss when positions of slot (distances) are varied from 2mm to 62mm. When the distance is at 2mm the notch performs at 2.36 GHz with -24.8 dB. By increasing the distance, the frequency will be shifted to the highest frequency. At the distance 32mm, the frequency is at 4.38 GHz with -29.12 dB. Meanwhile, for the insertion loss, the frequency at 2.36 GHz is -6dB and at 4.38 GHz, it is -8 dB. At the lowest frequency, it shows a better insertion loss compared to the highest frequency.

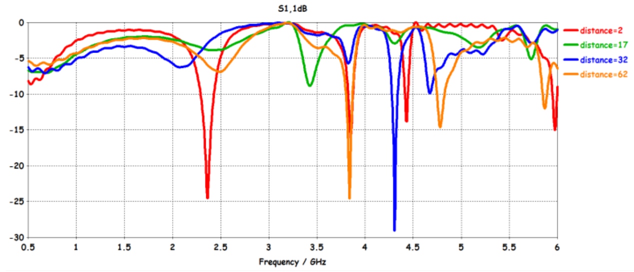

(a) Return Loss

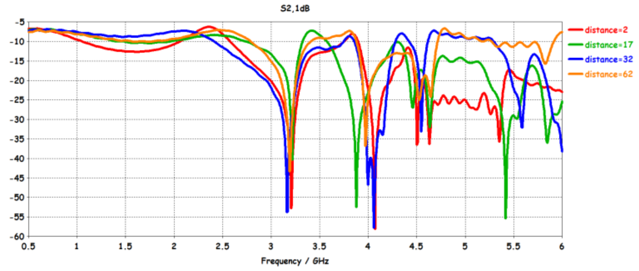

(b) Insertion Loss

Figure 5: Parametric study of S-parameter for distance of rectangular slot

B. *Width of Rectangular Slot*

Figure 6 illustrates the responses to return loss and insertion loss when the width of slot (W1) changes from 1mm to 5mm. From the figure, it clearly shows when the width increases it will widen the bandwidth at frequency 4.5 GHz to 5.5 GHz and others frequency slightly unchanged. But, the responses of insertion loss remains unchanged at frequency 4.5 GHz to 5.5 GHz even though the width of slot varies.

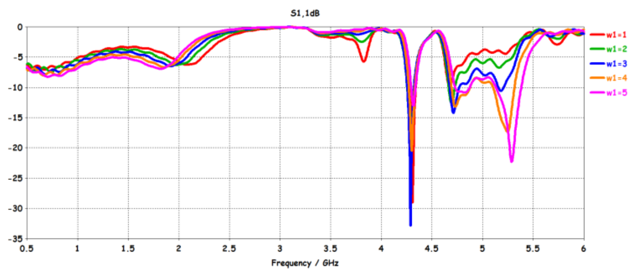

(a) Return Loss

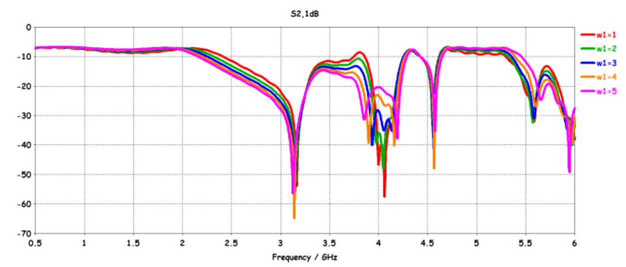

(b) Insertion Loss

Figure 6: Parametric study of S-parameter for width of rectangular slot

C. *Length of Rectangular Slot*

Figure 7 illustrates the results of the return loss and insertion loss for the variation of the lengths of slot (L1). At the frequency of 3.8 GHz the return loss will degrade near to -10 dB once the length of slot increases from 2mm to 4mm. Next, the length of slot increases to 8mm and 10mm will be shifted to about 400 MHz toward 4.3 MHz. The insertion loss at a frequency of 4.5 GHz to 5.5 GHz is unstable when the lengths of slot changes to 10mm. At a low frequency, the insertion loss is unchanged when the length of slot is varied. The increase of the length of slot (L1) is affected more at a high-frequency region.

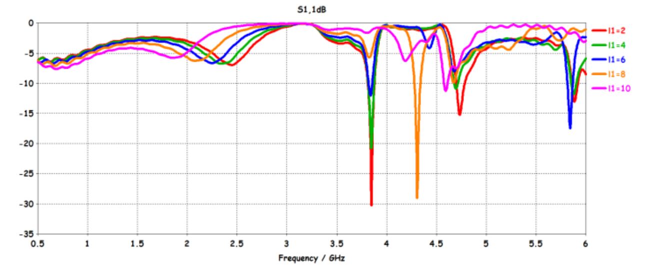

(a) Return Loss

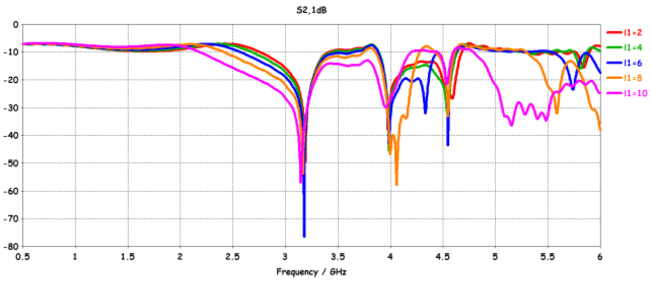

(b) Insertion Loss

Figure 7: Parametric study of S-parameter for rectangular slot

D. *Optimum Result*

The 1x4 Power Combiner with the rectangular slot is designed and simulated using a CST Microwave Studio. Figure 8(a) shows the result of return loss and insertion loss for port 1. The figure shows that the multiband occurs at high frequency and at low frequency and the return loss is slightly near to -10 dB. At the frequency of 3.1 GHz the insertion loss is dropped to -58.24 dB but it increases near to -3 dB when the frequency is at 5 GHz. All the insertion loss responses for others port are symmetrical because Port 1 is at the center of the patch. Figures 8(b), 8(c), 8(d) and 8(e) show the results of return loss and insertion for Port 2, Port 3, Port 4 and Port 5. Each port shows a return loss response at the frequency 3.8 GHz with -13.2 dB and multiband at high frequency. The transmission results for S23, S32, S45 and S54 are much better than the other transmissions responses. At 4.5 GHz until 5.5 GHz the responses are near to –2 dB. Next, the transmission responses for S12, S13, S14 and S15 are similar. The highest insertion loss is 62.29 dB at the frequency of 3.1 GHz and the lowest insertion loss is -4.7 dB at the frequency of 4.7 GHz.

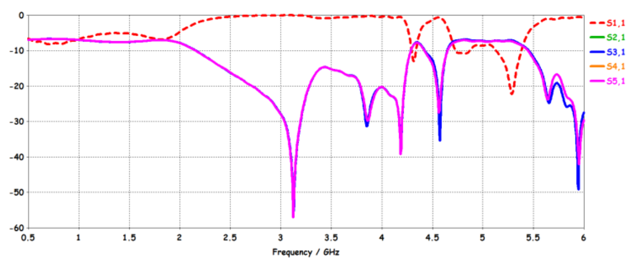

(a) Port 1

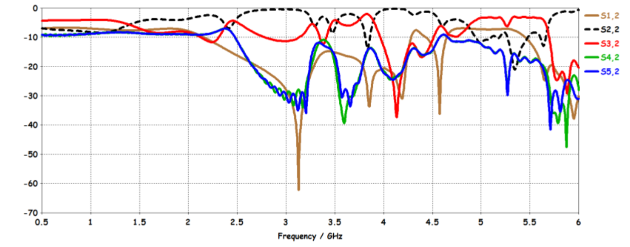

(b) Port 2

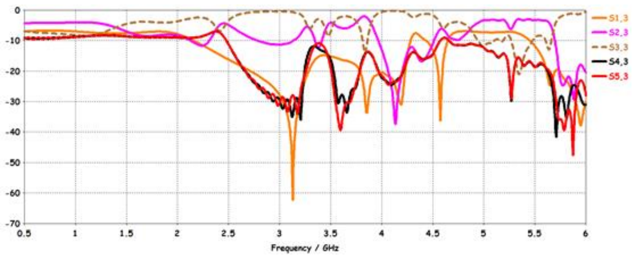

(c) Port 3

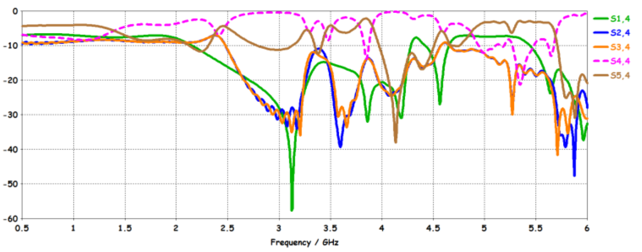

(d) Port 4

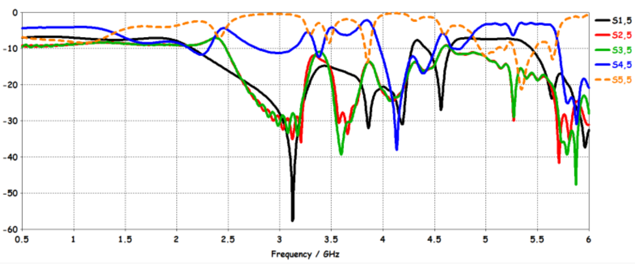

(e) Port 5

Figure 8: S-parameter for 1x4 Power Combiner with Rectangular Slot

IV. CONCLUSION

The 1x4 power combiner with the rectangular slot is designed and simulated in this paper at 0.5 GHz until 6 GHz. The changes of slot position will shift the response from low frequency to the highest frequency. Then the variation width of slot will widen the bandwidth at certain frequencies and the length of slot will improve the return loss. For future study, this design could be fabricated and the measurement result can be used to make a comparison with the simulation result.

ACKNOWLEDGMENT

The authors would like to thank Universiti Teknikal Malaysia Melaka (UTeM) and Ministry of Higher Education (MOHE) for support in obtaining the information and material in the development of our work. We also thank the anonymous referees whose comments led to an improved presentation of our work.

REFERENCES

[1] K. Song, S. Hu, Q. Xue and Y. Fan. 2012 . Compact U-band 32-way ring-cavity spatial power combiner with low insertion loss. Electronics Letters.

[2] Zhang, Lei., Zhu, Xiaowei., and Zhai, Jianfeng. 2012. Design of wideband planar power dividers/combiners. IEEE MTT-S International Microwave Workshop Series on Millimeter Wave Wireless Technology and Applications, IMWS.

[3] Chen, Mingyong. and Dou, Wenbin. 2009. A W-band Quasi-Optical Power Combiner Based on Waveguide Lens. IEEE Transactions on Microwave Theory and Techniques.

[4] N. S. Cheng, A. Alexanian, M. G. Case, and R. A. York, “20-W spatial power combiner in waveguide,” in IEEE MTT-S Int. Microwave Symp. Dig., Baltimore, MD, June 8–12, 1998.

[5] N.-S. Cheng, A. Alexanian, M. G. Case, and R. A. York, “20-W spatial power combiner in waveguide,” in IEEE MTT-S Int. Microwave Symp. Dig., Baltimore, MD, June 8–12, 1998.

[6] “Waveguide-based spatial power combining array and method for using the same,” U.S. Patent 5 736 908, April 7, 1998.

[7] “Broad-band spatially combined amplifier array using tapered slot transitions in waveguide,” IEEE Microwave Guided Wave Lett., vol. 7, pp. 42–44, Feb. 1997.

[8] A. Alexanian and R. A. York, “Broad-band waveguide-based spatial combiner,” in IEEE MTT-S Int. Microwave Symp. Dig., Denver, CO, June 8–13, 1997.

[9] Nai-Shuo Chen, Angelos Alexanian Michael G. Case. David B. Rensch, and Robert A. York. 40-W CW Broad-Band Spatial Power Combiner Using Dense Finline Arrays. IEEE Transactions on Microwave Theory And Techniques, Vol. 47, NO. 7, July 1999.

[10] Henyey, Frank S. (1982). "Distinction between a Perfect Conductor and a Superconductor". Phys. Rev. Lett. 49

[11] Peng Fei, Yong-Chang Jiao, Wei Hu, Fu-Shun Zhang. A miniaturized ant ipodal Vivaldi antenna with improved radiat ion characterist ics. IEEE Antennas and Wireless Propagation Letters, vol.10, pp. 127-130, 2011.

[12] U.A.Bakshi, A.V. Bakshi. 2010. Element of Electrical Engineering. Page 2-9

[13] Yang, Liang., Guo, Huiping., and Liu, Xueguan. 2010. An antipodal Vivaldi antenna for ultra-wideband system. IEEE International Conference on Ultra-Wideband, ICUWB2010 – Proceedings

[14] S. P. Bingulac, “On the compatibility of adaptive controllers (Published Conference Proceedings style),” in *Proc. 4th Annu. Allerton Conf. Circuits and Systems Theory*, New York, 1994, pp. 8–16.

[15] G. R. Faulhaber, “Design of service systems with priority reservation,” in *Conf. Rec. 1995 IEEE Int. Conf. Communications,* pp. 3–8.

[16] W. D. Doyle, “Magnetization reversal in films with biaxial anisotropy,” in *1987 Proc. INTERMAG Conf.*, pp. 2.2-1–2.2-6.